ChemComm

Accepted Manuscript

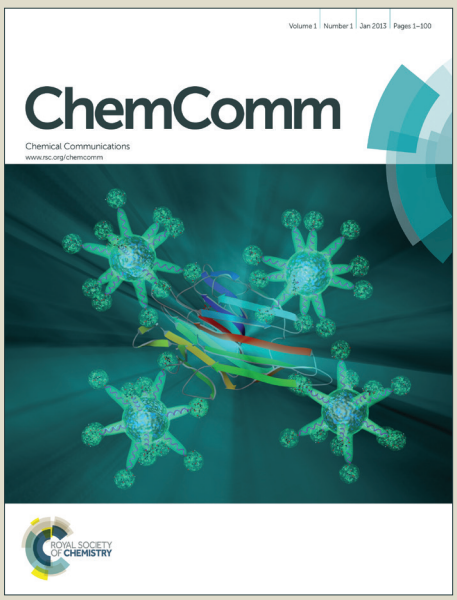

ROYAL SOCIETY OF CHEMISTRY

www.rsc.org/chemcomm

Cite this: DOI: 10.1039/c0xx00000x

www.rsc.org/xxxxxx

ARTICLE TYPE

A Nile Blue Based Infrared Fluorescent Probe: Imaging tumors that over-express Cyclooxygenase-2

Benhua Wang[a], Jiangli Fan[*a], Xianwu Wang[b], Hao Zhu[a], Jingyun Wang[*b], Huiying Mu[a], Xiaojun Peng[a]

Received (in XXX, XXX) Xth XXXXXXXXX 200XX, Accepted Xth XXXXXXXXX 200XX

DOI: 10.1039/b000000x

The first Golgi-localized cyclooxygenase-2 (COX-2)-specific near-infrared (NIR) fluorescence probe, , able to detect cancer cells was designed. Importantly, Niblue-C6-IMC preferentially labeled the tumors in mouse tumor model with deep tissue penetration capacity. It may be a promising molecular tool for guiding tumor resection during surgery.

Cancer is a major public health problem. Although progress has been made in reducing incidence and mortality rates, cancer still causes numerous deaths worldwide.[1-2] Therefore, the early diagnosis and treatment of cancer are particularly important. At present, cancer diagnostic methods include magnetic resonance imaging (MRI), ultrasound, positron emission tomography (PET) imaging, X-ray imaging and single-photon emission computed tomography (SPECT).[3-5] However, each of these methods has its drawbacks, such as limited spatial resolution of ultrasound[6], high instrument cost and radiological hazards[4] resulting from PET, SPECT and X-ray imaging. Besides, these methods are often not effective until the middle and last-stage cancer.[7-8] The main treatment protocols are extensive surgical resection, along with chemotherapy and radiotherapy.[9-10] When performing surgery, the accurate localization and adequate visualization of tumors are vital in optimizing surgical resection.[11] Failure to adequately recognize tumor margins and an incomplete resection may increase tumor recurrence and decrease survival rate.[12-13] Fluorescence imaging, serving as an alternative low-cost approach with relatively low toxicity, high sensitivity and resolution, noninvasive real-time capabilities, has become a powerful technique for the localization and dynamic monitoring of biomolecules in living systems.[14-17] Because the overexpressed enzymes are promising candidates of cancer-imaging target, the development of enzyme-activatable probes that report the species associated with cancer cells will allow for the discrimination of diseased and healthy tissue.[8, 18-19]

Cyclooxygenases (COXs) regulate the synthesis of prostaglandins and play an important role in tumor development and progression.[5, 20] Among the COXs, COX-1 is widely distributed and constitutively expressed in all tissues, whereas COX-2 is absent or expressed at very low levels in most normal cells, but is found at high levels in inflammatory lesions and many types of tumors.[20-24] Clinical data suggest that the overexpression of COX-2 promotes tumor growth, angiogenesis, and metastasis of cancer cells.[25-26] Recently, Uddin *et al.*[27] studied the selective inhibition of COX-2 using diverse fluorescent conjugates of COX-2 inhibitors. They[22] also reported a promising fluorescence method using COX-2-specific molecular probes. Zhang *et al.*[24, 28] discovered two fluorescent probes based on COX-2 as the cancer-imaging target. One of the probes specially targeted the Golgi apparatus, and the other discriminated tumors from inflammatory lesions. However, the absorption and emission wavelengths of these probes were short, thus limiting their application to a certain extent. Near-infrared (NIR) light (650–900 nm) has several advantages such as minimum photodamage to biological samples, minimal interference from background autofluorescence, and acceptable penetration of the fluorescent light through biological tissues.[29-30] NIR optical imaging offers great potential for the noninvasive detection of cancer sites *in vivo*; therefore, it is suitable for the wide exploration of possible clinical utility warranted.[31-32] Consequently, innovative strategies for the development of NIR fluorescent probes for bioimaging are actively sought after.

In this study, we report a novel COX-2-specific fluorescent probe, **Niblue-C6-IMC**, in which indomethacin (IMC) is linked to Nile Blue dye using a hexanediamine linker (Scheme 1). The probe has advantages of optical properties with NIR absorption (630 nm) and emission (670 nm) and can detect cancer cells by fluorescence imaging method. Instant and complete activation of the probe make it possible to use in the study of cancer progression and surgical resection procedures.

Nile Blue dye was selected as the fluorophore because of its distinguished properties such as NIR excitation and emission wavelengths, a high fluorescent quantum yields and a large absorption coefficient.[33-35] COX-2 was selected as the cancer-imaging target because it is overexpressed in most cancer cell lines. Uddin *et al.*[27] confirmed that IMC conjugates bound most tightly and selectively to COX-2. When selecting a linear hexanediamine as the linker, on the one hand, the long alkyl chain allows the IMC functionality to fully insert into the binding pocket of COX-2; on the other hand, the side-effect of the fluorophore on IMC is avoided. The spectroscopic properties of **Niblue-C6-IMC** in different solutions are summarized in Figure S1 and Table S1. The detailed synthetic route is described in Scheme 1. Both **Niblue-C6-IMC** and the intermediates were well characterized by ^{1}H NMR, ^{13}C NMR, and time-of-flight mass spectrometry (TOF-MS) (See the Supporting Information and Fig. S9–S17). To elucidate the mechanism of the fluorescence "off–on" process, the Gaussian 09 (DFT at the B3LYP/6-31G level) was used to calculate the frontier molecular orbital

energies. The oscillator strength of HOMO to LUMO transition was only 0.033, indicating that the electron transition from HOMO to LUMO is prohibited (Fig. S2). The calculated results show photoinduced electron transfer (PET) between Nile Blue and IMC; therefore, the fluorescence is quenched. In the presence of COX-2, **Niblue-C6-IMC** binds to three amino acids of COX-2, namely, Arg120, Tyr355, and Glu522, and the IMC moiety can be held by the large hydrophobic cavity of COX-2s' homodimer.[24, 28] We assume that the probe can adopt the unfolded conformation, resulting in the suppression of PET; thus, the fluorescence can be restored.

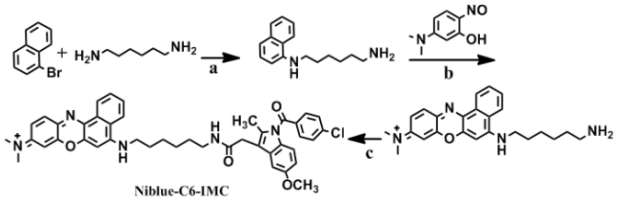

Scheme1. Synthesis route of **Niblue-C6-IMC**. Reagents and conditions: a) 2-methoxyethanol, CuI, $CsCO_3$,125 °C, 24 h ; b) ethanol, 90 °C, 2.5 h; c) DMF, EDCl, HOBt·H_2O, DMAP, rt, 24 h.

First, we evaluated whether **Niblue-C6-IMC** can specifically target COX-2 by native polyacrylamide gel electrophoresis (Native-PAGE) analysis. MCF-7 cancer cells, with high endogenous COX-2 levels, were treated with **Niblue-C6-IMC** (0–10 μM) *in situ* for 30 min, followed by in-gel fluorescence analysis. The analysis (Fig. 1) demonstrated that a fluorescent band appeared in the gel, consistent with purified COX-2; moreover, the intensity was concentration-dependent. In contrast, the pretreatment of cells with celecoxib, one of the potent reagents to control the active site of COX-2 in cancer cells, [28, 36] resulted in much weaker fluorescence. These data clearly indicate that the specific conjugation of **Niblue-C6-IMC** to the COX-2 structure significantly turned on the fluorescence, which inspired us to use this probe for potential applications in biological samples containing multiple COX-2.

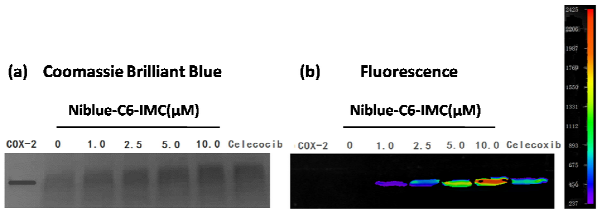

Fig. 1 Native-PAGE analysis of **Niblue-C6-IMC** labeling. (a) Coomassie Brilliant Blue staning and (b) fluorescence image with excitation λ= 630 nm. Lane 1: purified Cyclooxygenases-2; Lane 2-6: protein extracts of MCF-7 cells incubated with various concentrations of **Niblue-C6-IMC** for 30 min; Lane 7: protein extracts of MCF-7 cells preincubated with 13.0 μM celecoxib for 3 h, and then the addition of 5 μM **Niblue-C6-IMC** for another 30 min.

Next, enzyme-linked immunosorbent assay (ELISA) was used to determine the amount of COX-2 in different cell lines. The results (Fig. 2C) indicate that COX-2 is highly expressed in cancer cell lines (MCF-7 cell, 3.759 μg/mL; HepG2 cell, 3.590 μg/mL; Hela cell, 2.131 μg/mL), while minimally expressed in normal cell lines (COS-7 cell, 0.0075 μg/mL; LO-2 cell, 0.0145 μg/mL; OB cell, 0.0175 μg/mL). Then, these cell lines were incubated with 2.5 μM **Niblue-C6-IMC** for 30 min and imaged using a confocal fluorescence microscope. Both the cancer cell lines showed strong fluorescence; in contrast, all the COX-2-negative normal cell lines showed negligible fluorescence upon excitation at 635 nm (Fig. 2A). The fluorescence intensity (Fig. 2B) correlated with the concentration of COX-2 in these cell lines, which was measured by ELISA (Fig. 2C). These results indicate that **Niblue-C6-IMC** was cell membrane permeable and capable of distinguishing cancer cells from normal cells by labeling overexpressed COX-2 in cancer cells. Moreover, **Niblue-C6-IMC** strongly stained cancer cells within 30 min, and the fluorescence intensity remained almost unchanged after prolonged incubation time (120 min). However, the normal cells still maintained the minimal signal during the long incubation time (Fig. S3). The time scan results indicate that **Niblue-C6-IMC** served as a NIR marker for long-time observations in living cancer cells.

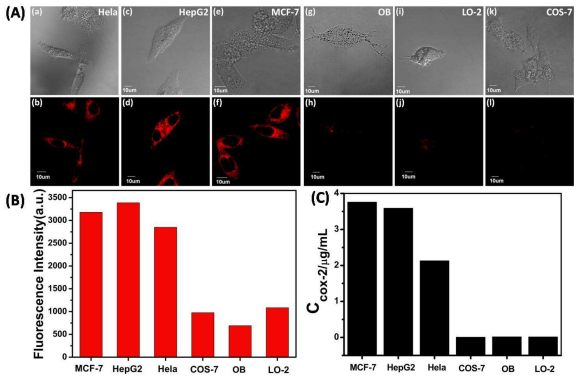

Fig. 2 (A) Living cells staining with **Niblue-C6-IMC** (2.5 μM). a, c, e, g, i and k are white light images, b, d, f, h, j and l are fluorescence images. Excitation wavelength = 635 nm, scan range = 640-700 nm; (B) Quantitative analysis of fluorescence responds of **Niblue-C6-IMC**; (C) Content of COX-2 in different cells by ELISA.

To evaluate whether **Niblue-C6-IMC** specifically targeted COX-2, HepG2 cells were preincubated with 0, 6.5, or 13.0 μM celecoxib. The fluorescence intensity (670 ± 10 nm) decreased gradually with increasing amount of celecoxib (Fig. 3), because celecoxib prevented the labeling of HepG2 cells by **Niblue-C6-IMC**. Similar results (see Fig. S4) were also obtained in Hela and MCF-7 cells. And as shown in Fig. 4, the activity of COX-2 gradually decreased with increasing probe concentration, and a good linearity relationship was obtained. The IC50 value of **Niblue-C6-IMC** for COX-2 was 0.71 μM, which is very close to the IC50 value of IMC for COX-2[28] (0.75 μM), indicating that the binding affinity of **Niblue-C6-IMC** for COX-2 is as strong as that of IMC. Collectively, these data confirmed that **Niblue-C6-IMC** serves as a potent and selective fluorescent inhibitor for COX-2 in cancer cells.

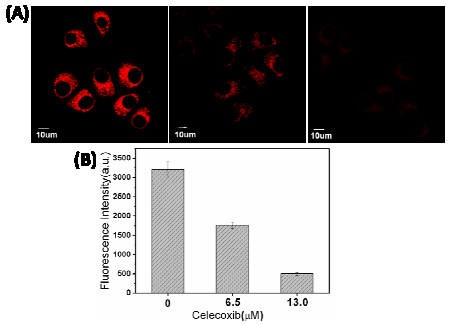

Fig. 3 Labeling of COX-2-expressing cells by **Niblue-C6-IMC**. (A) HepG2 cells pretreated with 0, 6.5, or 13.0 μM celecoxib for 3 h prior to **Niblue-C6-IMC** treatment. Excitation wavelength = 635 nm, scan range = 640-700 nm; (B) Quantitative image analysis of the average total fluorescence of HepG2 cells, determined from analysis of 10 cells in each sample image.

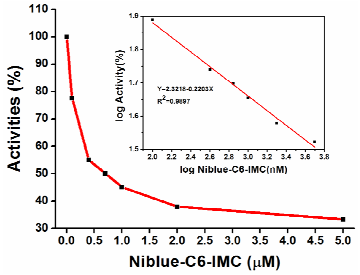

Fig. 4 Dose-inhibition curves of **Niblue-C6-IMC** (0-5.0 μM) on COX-2. The activity of COX-2 was measured by enzyme-linked immunosorbent assay.

It has been reported that the Golgi apparatus actively involved in the initiation and execution of cellular demise, which results in COX-2 accumulating in the Golgi apparatus.[24, 37] A well-known fluorescent probe for the Golgi apparatus, NBD C6-ceramide, was used to costain MCF-7, Hela and HepG2 cells respectively with **Niblue-C6-IMC** to determine its subcellular distribution. The fluorescence images (Fig. 5a, Fig. 5d and Fig. S5a) stained by **Niblue-C6-IMC** match well with those stained by NBD C6-ceramide (Fig. 5b, Fig. 5e and Fig. S5b). The colocalization coefficients were evaluated by Pearson's correlation factor[38], which is 0.96, 0.97 and 0.93 respectively, indicating that **Niblue-C6-IMC** can mark the Golgi apparatus clearly in cancer cells with a very high efficiency.

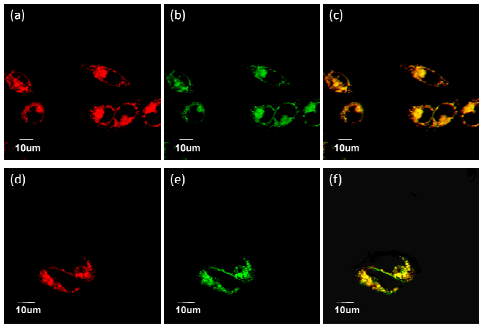

Fig. 5 Fluorescence images of **Niblue-C6-IMC** (2.5 μM) in MCF-7 (a-c) and Hela (d-f) cells costained with NBD C6-ceramide (5.0 μM). (a) and (d): red emission from **Niblue-C6-IMC**, excitation wavelength = 635 nm, scan range = 640-700 nm. (b) and (e): green emission from NBD C6-ceramide, excitation wavelength = 488 nm, scan range = 500-540 nm. (c) and (f): overlay of the red and green channels.

Flow cytometry (FCM) enables the rapid measurement of fluorescence intensity for multiple cell populations.[39] To further confirm that the probe can efficiently label COX-2, **Niblue-C6-IMC**-labeled cells were studied quantitatively by flow cytometry. Cells were incubated in 2.5 μM **Niblue-C6-IMC** for 30 mins, and then the fluorescence was measured using primarily flow cytometry (λ_{ex} = 633 nm, λ_{em} = 670 nm) in 10,000 individual cells. Normal cells (COS-7 and OB) were used as the negative controls. As shown in Fig. S6, high intensity fluorescence signals were obtained for **Niblue-C6-IMC** in the cancer cells (MCF-7 and Hela), and >95 % cells could be selected by the dye, whereas the non-cancer cell lines produced a little fluorescence compared with the cancer cell lines. Therefore, **Niblue-C6-IMC** can be used as a potential visual tool to selectively label cancer cells. Since low cytotoxicity is one of the key criteria for general cancer detection, the cytotoxicity of **Niblue-C6-IMC** to MCF-7 cells was evaluated via the MTT test. Fig. S7 shows that after 24 h of the cellular internalization of 2.5 μM **Niblue-C6-IMC**, >92 % of the cells survived, thus making **Niblue-C6-IMC** suitable for microscopy imaging applications in living specimens under the experimental conditions.

To further assess **Niblue-C6-IMC** as a NIR fluorescent probe for bioimaging applications, we primarily investigated the applicability of this probe for tissue imaging. After the incubation of cancerous and normal liver tissue slices with 30 μM **Niblue-C6-IMC** for 30 min at 37 °C, the fluorescence images were obtained with 635 nm excitation. Significantly, the cancerous tissues revealed a strong fluorescence signal; in contrast, only weak or negligible signals were detected in normal liver tissue slices (Fig. S8). Therefore, the probe could distinguish cancerous tissues from normal tissues by fluorescence imaging.

Finally, the ability of **Niblue-C6-IMC** in COX-2-targeted cancer imaging was studied using a mouse tumor model. The tumor-bearing nude mice were dosed by subcutaneous injection with 100 μM **Niblue-C6-IMC**. When a Small Animals Living Imaging System was used with an excitation wavelength of 630 nm and an emission wavelength of 700 nm, strong fluorescence signal was detected in the COX-2 expressing MDA-MB-231 tumor after 1 h (Fig. 6b). We normalized **Niblue-C6-IMC** signals in the tumor area (T, right flank) with that in the normal area (N, same ROI in left flank) to generate tumor-to-normal (T/N) ratios as high as 9.4. These results support the hypothesis that **Niblue-C6-IMC** has potential for applications in living systems by selective accumulation in tumor lesions. Further, a COX-2 blocking experiment was performed, in which the nude mice with MDA-MB-231 xenografts were pretreated with celecoxib in PBS by subcutaneous injection prior to the dosing of **Niblue-C6-IMC**. After 1 h post injection, the celecoxib-pretreated mice showed weak fluorescence signals in tumors (Fig. 6d) and a significantly lower T/N ratio of roughly 4.1. Thereby, celecoxib partially inhibited the activity of COX-2, thus reducing the tumor uptake of **Niblue-C6-IMC** *in vivo*. In other words, this indicated that **Niblue-C6-IMC** labelled the tumor site by specifically binding with COX-2. These results confirm that **Niblue-C6-IMC** is an important NIR probe for cancer imaging.

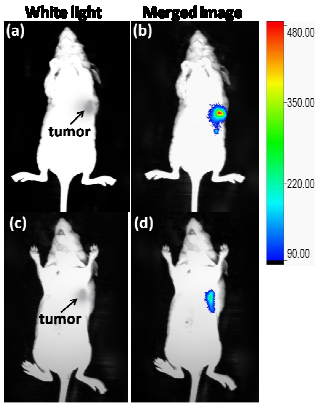

Fig. 6 In vivo tumor optical imaging and competitive blocking studies. (a) and (c) were white lights of nude mice with the MDA-MB-231 tumor. (b) Mice were treated with **Niblue-C6-IMC** (100 μM) dissolved in 200 μL of PBS via the subcutaneous injection. The incubation times were 60 min. (d) Nude mice were pre-dosed with 520 μM celecoxib for 60 min, and then injected 100 μM **Niblue-C6-IMC** for another 60 min. The mice were imaged using a NightOWL II LB983 small animal in vivo imaging system with an excitation filter of 630 nm and an emission filter of 700 nm. Images are representative of replicate experiments (n = 3).

Conclusions

In summary, we report the first COX-2-specific NIR fluorescent probe, **Niblue-C6-IMC**, for visualizing tumor sites in cancer cells and *in vivo*. In COX-2 negative normal cells, the fluorescence of **Niblue-C6-IMC** was weak, while its fluorescent signal was selectively and quickly generated by interacting with COX-2 accumulated in the Golgi apparatus of cancer cells. The "off–on" fluorescence enhancement results from the inhibition of PET following the **Niblue-C6-IMC** binding to COX-2. Simultaneously, the probe could be used to screen cancer cells in a rapid, sensitive, and quantitative manner using flow cytometry. Because NIR optical imaging offers great potential for the noninvasive detection of cancer sites in vivo, the probe may have applications ranging from an accurate cancer diagnosis to guiding tumor resection during surgery.

We thank Dr. Fang Chen at the Dalian University of Technology for providing HepG2 cells and technical advice. This work was financially supported by NSF of China (21136002, 21376039, 21422601, 21421005 and 21104008), National Basic Research Program of China (2013CB733702), Ministry of Education (NCET-12-0080) and Fundamental Research Funds for the Central University (DUT14ZD214).

Notes and references

[a] *State Key Laboratory of Fine Chemicals, Dalian University of Technology, No. 2 Linggong Road, High-tech District, Dalian 116024, China. Fax: +86 411 84986306; Tel: +86 411 84986327; E-mail: fanjl@dlut.edu.cn*

[b] *Department School of Life Science and Biotechnology, Dalian University of Technology, No. 2 Linggong Road, Ganjingzi District, Dalian 116024, China. Fax: +86 411 84706365; Tel: +86 411 84706355; E-mail: wangjingyun67@dlut.edu.cn*

† Electronic Supplementary Information (ESI) available: [details of any supplementary information available should be included here]. See DOI: 10.1039/b000000x/

1. R. Siegel, D. Naishadham and A. Jemal, *CA-Cancer. J. Clin.*, 2012, **62**, 10-29.
2. J. Li, F. Liu, Q. Shao, Y. Min, M. Costa, E. K. L. Yeow and B. Xing, *Adv. Healthc. Mater.*, 2014, **3**, 1230-1239.
3. S. L. Gibbs, *Quant. Imaging. Med. Surg.*, 2012, **2**, 177-187.
4. L. Fass, *Mol. Oncol.*, 2008, **2**, 115-152.
5. H.-L. Huang, C.-N. Yeh, W.-Y. Lee, Y.-C. Huang, K.-W. Chang, K.-J. Lin, S.-F. Tien, W.-C. Su, C.-H. Yang, J.-T. Chen, W.-J. Lin, S.-S. Fan and C.-S. Yu, *Biomaterials*, 2013, **34**, 3355-3365.
6. Q. T. Nguyen, E. S. Olson, T. A. Aguilera, T. Jiang, M. Scadeng, L. G. Ellies and R. Y. Tsien, *Proc. Natl. Acad. Sci.*, 2010, **107**, 4317-4322.
7. E. F. J. de Vries, J. Doorduin, R. A. Dierckx and A. van Waarde, *Nucl. Med. Biol.*, 2008, **35**, 35-42.
8. Y. Urano, M. Sakabe, N. Kosaka, M. Ogawa, M. Mitsunaga, D. Asanuma, M. Kamiya, M. R. Young, T. Nagano, P. L. Choyke and H. Kobayashi, *Sci. Transl. Med.*, 2011, **3**, 110-119.
9. W. Stummer, H.-J. Reulen, T. Meinel, U. Pichlmeier, W. Schumacher, J.-C. Tonn, V. Rohde, F. Oppel, B. Turowski, C. Woiciechowsky, K. Franz, T. Pietsch and A.-G. S. Group, *Neurosurgery*, 2008, **62**, 564-576.
10. J. P. Belloch, V. Rovira, J. L. Llácer, P. A. Riesgo and A. Cremades, *Acta. Neurochir.*, 2014, **156**, 653-660.
11. Y. Hiroshima, A. Maawy, S. Sato, T. Murakami, F. Uehara, S. Miwa, S. Yano, M. Momiyama, T. Chishima, K. Tanaka, M. Bouvet, I. Endo and R. M. Hoffman, *J. Surg. Res.*, 2014, **187**, 510-517.
12. R. De la Garza-Ramos, M. Bydon, M. Macki, J. Huang, R. J. Tamargo and A. Bydon, *Neurol. Res.*, 2014, **36**, 928-938.
13. S. Keereweer, P. B. Van Driel and C. W. Lowik, *Mol. Imag. Biol.*, 2014, **16**, 10-12.
14. T. Harada, K. Sano, K. Sato, R. Watanabe, Z. Yu, H. Hanaoka, T. Nakajima, P. L. Choyke, M. Ptaszek and H. Kobayashi, *Bioconjugate Chem.*, 2014, **25**, 362-369.
15. M. Bio, P. Rajaputra, G. Nkepang and Y. You, *J. Med. Chem.*, 2014, **57**, 3401-3409.
16. H. Lee, J. Kim, H. Kim, Y. Kim and Y. Choi, *Chem. Comm.*, 2014, **50**, 7507-7510.
17. A. A. Neves and K. M. Brindle, *BBA-Rev. Cancer*, 2006, **1766**, 242-261.
18. W. C. Silvers, B. Prasai, D. H. Burk, M. L. Brown and R. L. McCarley, *J. Am. Chem. Soc., 2012, **135**, 309-314.*
19. S. Luo, E. Zhang, Y. Su, T. Cheng and C. Shi, *Biomaterials*, 2011, **32**, 7127-7138.
20. C. Denkert, K.-J. Winzer, B.-M. Müller, W. Weichert, S. Pest, M. Köbel, G. Kristiansen, A. Reles, A. Siegert, H. Guski and S. Hauptmann, *Cancer*, 2003, **97**, 2978-2987.
21. R. Gautam, S. M. Jachak, V. Kumar and C. G. Mohan, *Bioorg. Med. Chem.Lett.*, 2011, **21**, 1612-1616.
22. M. J. Uddin, B. C. Crews, A. L. Blobaum, P. J. Kingsley, D. L. Gorden, J. O. McIntyre, L. M. Matrisian, K. Subbaramaiah, A. J. Dannenberg, D. W. Piston and L. J. Marnett, *Cancer Res.*, 2010, **70**, 3618-3627.
23. P. Vitale, S. Tacconelli, M. G. Perrone, P. Malerba, L. Simone, A. Scilimati, A. Lavecchia, M. Dovizio, E. Marcantoni, A. Bruno and P. Patrignani, *J. Med. Chem.*, 2013, **56**, 4277-4299.
24. H. Zhang, J. Fan, J. Wang, S. Zhang, B. Dou and X. Peng, *J. Am. Chem. Soc.*, 2013, **135**, 11663-11669.
25. A. Thiel, J. Mrena and A. Ristimäki, *Cancer Metast. Rev.*, 2011, **30**, 387-395.
26. F. Wuest, T. Kniess, R. Bergmann and J. Pietzsch, *Bioorg. Med. Chem.*, 2008, **16**, 7662-7670.
27. M. J. Uddin, B. C. Crews, K. Ghebreselasie and L. J. Marnett, *Bioconjugate Chem.*, 2013, **24**, 712-723.
28. H. Zhang, J. Fan, J. Wang, B. Dou, F. Zhou, J. Cao, J. Qu, Z. Cao, W. Zhao and X. Peng, *J. Am. Chem. Soc.*, 2013, **135**, 17469-17475.
29. F. P. Verbeek, B. E. Schaafsma, Q. R. Tummers, J. R. van der Vorst, W. J. van der Made, C. I. Baeten, B. A. Bonsing, J. V. Frangioni, C. J. van de Velde and A. L. Vahrmeijer, *Surg. Endos.*, 2014, **28**, 1076-1082.
30. H. Takeyama, T. Hata, J. Nishimura, R. Nonaka, M. Uemura, N. Haraguchi, I. Takemasa, T. Mizushima, H. Yamamoto and Y. Doki, *Surg. Endos.*, 2014, **28**, 1984-1990.
31. M. Cui, M. Ono, H. Watanabe, H. Kimura, B. Liu and H. Saji, *J. Am. Chem. Soc.*, 2014, **136**, 3388-3394.
32. L. Zhu, Y. Ma, D. O. Kiesewetter, Y. Wang, L. Lang, S. Lee, G. Niu and X. Chen, *ACS Chem. Biol.*, 2014, **9**, 510-516.
33. J. Fan, H. Dong, J. Wang, H. Zhu, H. Zhang, X. Peng, M. Hu and W. Sun, *Chem. Commun.*, 2014, **50**, 882-884.
34. T. Guo, L. Cui, J. Shen, W. Zhu, Y. Xu and X. Qian, *Chem. Commun.*, 2013, **49**, 10820-10822.
35. A. A. Frick, F. Busetti, A. Cross and S. W. Lewis, *Chem. Commun.*, 2014, **50**, 3341-3343.
36. C. A. Rouzer and L. J. Marnett, *J. Lipid Res.*, 2009, **50**, 29-34.
37. D. Wlodkowic, J. Skommer, D. McGuinness, C. Hillier and Z. Darzynkiewicz, *Leukemia Res.*, 2009, **33**, 1440-1447.
38. P. Ahlgren, B. Jarneving and R. Rousseau, *J. Am. Soc. Inform. Sci. Technol.*, 2003, **54**, 550-560.
39. D. Sun, Y. Liu, Q. Yu, X. Qin, L. Yang, Y. Zhou, L. Chen and J. Liu, Biomaterials, 2014, **35**, 1572-1583.